Runge-Kutta discontinuous Galerkin method in solving compressible two-medium flow

***H. T. Lu[1], †N. Zhao[1]**

[1]College of Aerospace Engineering, Nanjing University of Aeronautics and Astronautics, Nanjing, Jiangsu 210016, P.R. China.

*Presenting author: lhtgkzy@126.com
†Corresponding author: nzhao2000@hotmail.com

Abstract

In this paper, the Runge-Kutta discontinuous Galerkin method is used in solving compressible two-medium flow. The material interface is explicitly tracked by the front tracking method and the interface boundary conditions are defined via the real ghost fluid method. Several numerical examples are presented to show the accuracy and capacity of this method. It is found that the mass errors are smaller compared to the results obtained by the same order accurate finite difference method.

Keywords: Runge-Kutta discontinuous Galerkin method, front tracking method, real ghost fluid method, mass errors.

Introduction

One major difficulty in solving compressible two-medium flow is how to treat the material interface accurately. The front tracking method [3] provides an explicit way to track the moving interface and a sharp interface boundary is maintained during the computation. The ghost fluid method (GFM) [2] introduced by Fedkiw et al. presents a simple and flexible way of treating the material interface. However, when the pressure or the velocity experiences a large jump across the interface, the GFM can lead to inaccuracy or even incorrect solution. To better consider the effect of wave interaction and material property, the real ghost fluid method (RGFM) [9] is proposed to update the real fluid states and obtain the ghost fluid states by defining a Riemann problem at the interface. With these ghost fluid states, the mediums can be solved separately as if it is in a single medium.

In recent years, the Runge-Kutta discontinuous Galerkin (RKDG) method [1] performed very well and has been broadly applied to the simulation of single medium flow. For the RKDG method, the higher accuracy is easily obtained in smooth region and we can get the numerical solution everywhere from the solution polynomials. In many earlier works, the basic scheme used to solve the compressible multimedium flow is usually finite difference method [4]. For higher order accurate finite difference method, more ghost fluid states across the interface are solved. Since the geometrical information far from the interface is not solved precisely by the front tracking method, the corresponding ghost fluid states are less accurate especially for the complex interface in the later stage evolution [5][6]. However, due to the good compactness of the RKDG method, we only need to define the ghost fluid states in the ghost fluid cells which have the common edges with the real fluid cells. This is very simple but also favorable. The intention of this work is to apply the RKDG method in the simulation of compressible two-medium flow and compare the mass errors obtained by the same order accurate finite difference method. The material interface is explicitly tracked by several connected marker points and the RGFM is used to define the interface boundary conditions. A Riemann problem is constructed in the normal direction of each marker point, and the Riemann solutions are used to advance the interface and obtain the ghost fluid states directly.

Equations and interface treatment

Governing equations

The two-dimensional hyperbolic conservation laws can be written as follows:

$$\frac{\partial \mathbf{U}}{\partial t} + \nabla \cdot \mathbf{F}(\mathbf{U}) = 0 \tag{1}$$

where $\mathbf{U} = [\rho, \rho u, \rho v, E]^T$, $\mathbf{F}(\mathbf{U}) = [\mathbf{F}_1(\mathbf{U}), \mathbf{F}_2(\mathbf{U})]$, $\mathbf{F}_1(\mathbf{U}) = [\rho u, \rho u^2 + p, \rho uv, (E+p)u]^T$, $\mathbf{F}_2(\mathbf{U}) = [\rho v, \rho uv, \rho v^2 + p, (E+p)v]^T$. Here ρ is the density, u and v are the velocities, p is the pressure, E is the total energy per unit volume. The total energy is given as:

$$E = \rho e + \rho(u^2 + v^2)/2 \tag{2}$$

where e is the internal energy per unit mass. The stiffened gas equation of state is used:

$$p = (\gamma - 1)\rho e - \gamma B \tag{3}$$

here γ and B are characteristic parameters of material and can be treated as constants. For the ideal gas γ represents the ratio of the specific heats and B is zero.

Interface tracking

As indicated in Fig. 1, medium 1 and medium 2 are separated by the material interface. The marker points are represented by the intersections of the interface and the grid lines. $\vec{N}$ is the normal vector and $\vec{T}$ is the tangential vector of each marker point. Point $A(x_A, y_A)$ and point $B(x_B, y_B)$ are obtained by the same distance Δn [3] from the marker point $P(x_P, y_P)$:

$$\Delta n = \left[\left(\frac{N_{Px}}{\Delta x} \right)^2 + \left(\frac{N_{Py}}{\Delta y} \right)^2 \right]^{-\frac{1}{2}} \tag{4}$$

$$\begin{aligned} x_A &= x_P - \Delta n \cdot N_{Px},\ y_A = y_P - \Delta n \cdot N_{Py} \\ x_B &= x_P + \Delta n \cdot N_{Px},\ y_B = y_P + \Delta n \cdot N_{Py} \end{aligned} \tag{5}$$

where $\vec{N}_P = (N_{Px}, N_{Py})$ is the unit normal vector of the marker point P and Δx and Δy are the cell sizes. A Riemann problem is constructed at the marker point P with the initial conditions:

$$\mathbf{U}_0 = \begin{cases} \mathbf{U}_A \\ \mathbf{U}_B \end{cases} \tag{6}$$

where $\mathbf{U}_A$ and $\mathbf{U}_B$ are the fluid states at point A and point B and can be solved from the solution polynomials directly in the RKDG method [1]. An approximate Riemann problem solver (ARPS) based on a two shock structure can be employed to obtain the Riemann solutions. We denote the Riemann solutions by $\mathbf{R}_P = [\rho_I^L, \rho_I^R, u_I^N, p_I]^T$, where the subscript "$I$" refers to the interface, and the superscript "L" and "R" denote the left and right side of the interface, respectively. The tangential velocity of the marker point P depends on the sign of the normal velocity and is defined as:

$$v_I^T = \begin{cases} v_A^T, & \text{if } u_I^N \geq 0 \\ v_B^T, & \text{otherwise} \end{cases} \tag{7}$$

where v_A^T and v_B^T are the tangential velocity of point A and point B, respectively. After the velocity of each marker point has been solved, its new position is updated simultaneously:

$$\vec{x}_f^{(1)} = \vec{x}_f^n + \Delta t \cdot \vec{v}_f(\vec{x}_f^n)$$
$$\vec{x}_f^{(2)} = \frac{3}{4}\vec{x}_f^n + \frac{1}{4}\vec{x}_f^{(1)} + \frac{1}{4}\Delta t \cdot \vec{v}_f(\vec{x}_f^{(1)}) \tag{8}$$
$$\vec{x}_f^{n+1} = \frac{1}{3}\vec{x}_f^n + \frac{2}{3}\vec{x}_f^{(2)} + \frac{2}{3}\Delta t \cdot \vec{v}_f(\vec{x}_f^{(2)})$$

where $\vec{x}_f^n$ and $\vec{x}_f^{n+1}$ are the positions of the interface at time t^n and t^{n+1}, respectively. $\vec{v}_f$ is the interface velocity, and Δt is the time step.

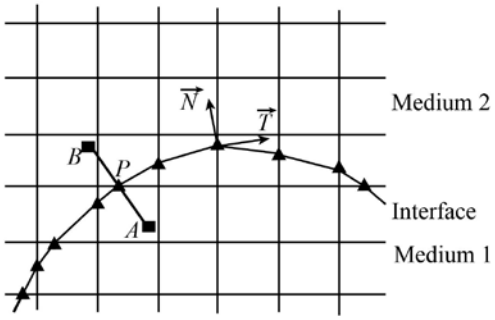

Figure 1. Construct the Riemann problem

RGFM

Since the Riemann problem has been solved at the marker point in the interface tracking, the Riemann solutions can be used directly to update the real fluid states and obtain the ghost fluid states. As shown in Fig. 2, points *R*, *S*, *P* and *Q* are the marker points near the grid cell *A*, $\vec{N}_P$ is the normal vector of the marker point *P* and $\vec{N}_A$ is the normal vector of the grid cell *A*. The flow states at the cell *A* can be updated by the marker point nearby. The marker point *P* is selected if the angle between $\vec{N}_P$ and $\vec{N}_A$ is the minimum compared with other marker points. We project the Riemann solutions at the marker point *P* to the base function space to obtain the average values in cell *A* while the tangential velocity in cell *A* remains unchanged. It is similar for other real fluid cells adjacent to the interface. The ghost fluid states are obtained by solving the advection equation:

$$\frac{\partial \phi}{\partial t} \pm \vec{N} \square \nabla \phi = 0 \tag{9}$$

where ϕ is the density, the normal velocity, the tangential velocity and the pressure, $\vec{N}$ is the unit normal vector of the ghost cells.

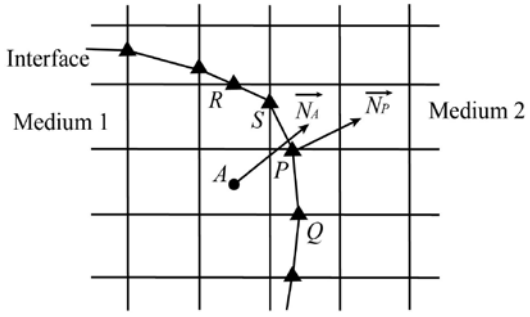

Figure 2. Update the fluid states adjacent to the interface

Numerical examples

In this section, several two dimensional compressible two-medium flow problems are simulated on uniform Cartesian meshes. The governing equations for each medium are solved by the P^2 (third-order accurate) RKDG method and the TVB limiter constant [1] is taken as 0.1. The time integration is solved by a third-order TVD Runge-Kutta scheme. The RKDG method combined with the front tracking method is named as RKDG-FT method for convenience.

Shock bubble interaction

The computational domain is shown in Fig. 3 and the geometrical parameters are: a=50 mm, b=25 mm, c=100 mm, d=325 mm, e=44.5 mm. A shock wave propagates to the left and hits a helium bubble with a Mach number of 1.22. Only the upper half domain is computed since the flow field is symmetric about the center axis. On the left and right boundaries, nonreflecting boundary condition is used and the upper boundary is treated as slip-wall. The speed of sound and the diameter of bubble are used for nondimensionalization. The computational domain is divided into 650×89 mesh cells. The initial conditions are: $\rho = 1, u = 0, v = 0, p = 1/1.4, \gamma = 1.4,$ for pre-shocked air, $\rho = 1.3764, u = -0.3336, v = 0, p = 1.5698/1.4,$ for post-shocked air, $\rho = 0.1819, u = 0, v = 0,$ $p = 1/1.4, \gamma = 1.648,$ for helium. The time histories of density field are shown in Fig. 4. The evolution of the bubble shape and the refracted shock wave can be seen clearly. In Fig. 5, it shows the space-time diagram for three characteristic points (Jet, Downstream, Upstream shown in the figure) with earlier results from [8]. In general, these results are in a relatively good agreement. To make quantitative comparisons with the finite difference method, here we replace the RKDG method by the third order accurate weighted essentially non-oscillatory (WENO) method and keep everything else unchanged in the code [4]. The WENO method combined with the front tracking method is named as WENO-FT method for convenience. The relative mass error of helium bubble is computed and shown in Fig. 6. It is found that the relative mass errors are limited within 7% before the helium bubble collapses for both methods. The general trends of the relative mass errors with time are similar but the error caused by the RKDG-FT method is much smaller.

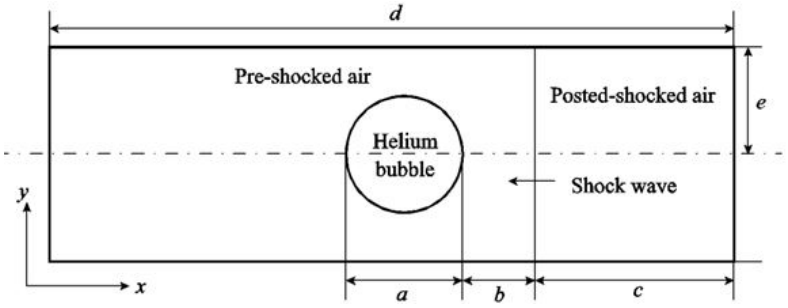

Figure 3. A schematic of computational domain (not to scale)

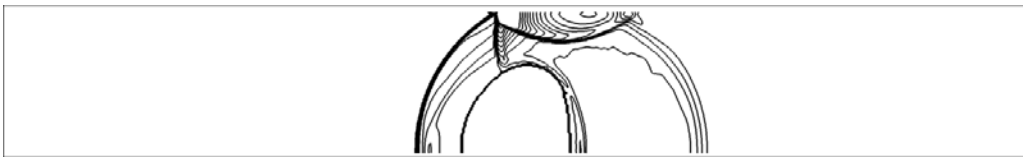

(a) t=102μsec

(b) t=427μsec

(c) t=674μsec

Figure 4. The evolution of density field (60 equally spaced density contours from 0.1 to 1.6)

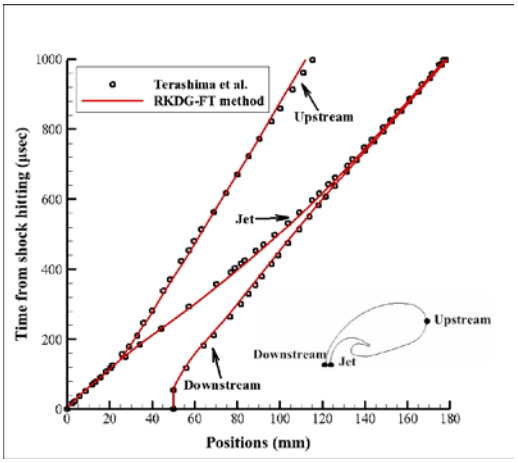

Figure 5. Space-time diagrams for three characteristic interface points

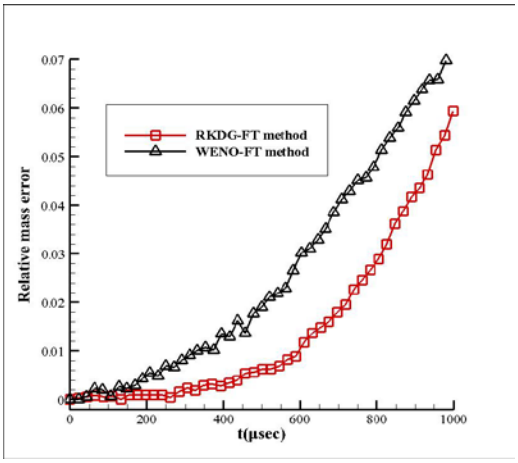

Figure 6. Comparison of relative mass error of helium bubble

Richtmyer-Meshkov instability

This example consists of two simulations of problems with gas-gas and gas-liquid interfaces. As indicated in Fig. 7, a computational domain of [0,4]×[0,0.5] is used and the initial location of the interface is represented by: $x = 2.9 - 0.1\sin(2\pi(y + 0.25)),\quad 0 < y < 0.5$. The upper and lower boundaries are periodic and the nonreflecting boundary condition is applied at the left and right boundaries. The computational domain is divided into 1000×125 mesh cells. The first one is a gas-

gas interface. At x=3.2 there is a planar shock wave with Mach number 1.24 in air propagating from the right to the left of the SF_6-air interface. The initial conditions are: $\rho = 5.04, u = 0, v = 0, p = 1,$ $\gamma = 1.093,$ for SF_6, $\rho = 1, u = 0, v = 0, p = 1, \gamma = 1.4,$ for pre-shocked air, $\rho = 1.411, u = -0.39,$ $v = 0, p = 1.628, \gamma = 1.4,$ for post-shocked air. The flow evolution in the density field is presented in Fig. 8. The interface is accelerated by a shock wave coming from the light-fluid to the heavy-fluid region. Fig. 9 presents the time evolution of the location of the spike and the leading edge of the bubble along with the results in [8]. It shows that these results are almost identical. The relative mass error of the SF_6 medium is shown in Fig. 10 before the shock wave transmits to the left boundary in order to make comparisons between the RKDG-FT method and the WENO-FT method. It is found that these errors are similar at the initial stage. Later, the error by the WENO-FT method increases quickly while the error curve by the RKDG-FT method is much smoother.

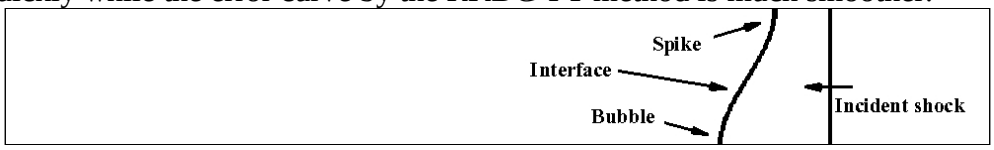

Figure 7. A schematic of flow field at t=0

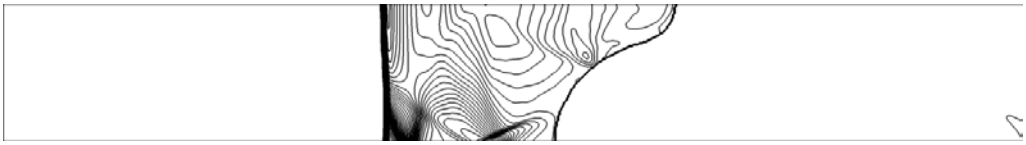

(a) t=2.3099

(b) t=4.6062

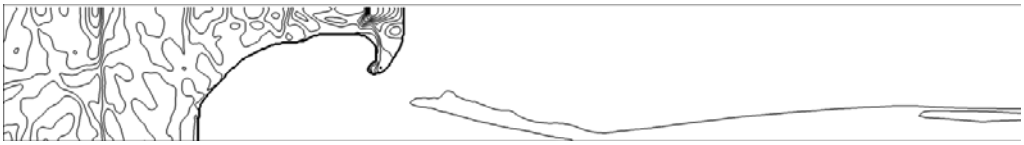

(c) t=6.9045

Figure 8. Density field (230 equally spaced density contours from 0.5 to 9.5)

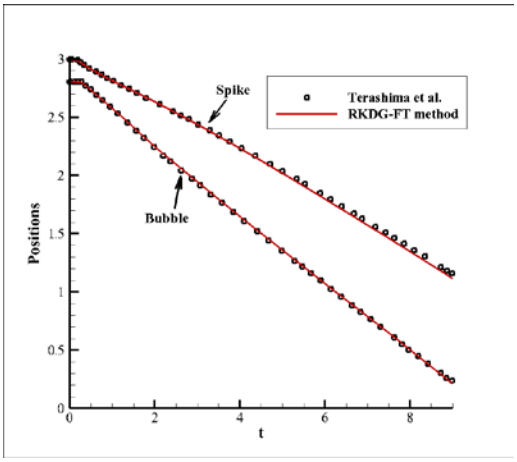

Figure 9. Comparison on time histories of characteristic positions

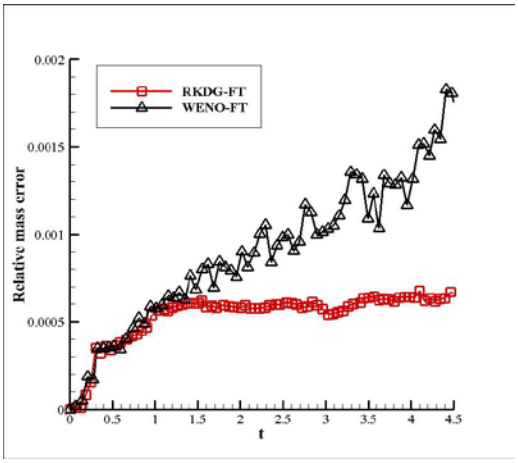

Figure 10. Comparison of relative mass error of SF_6

The second one is a gas-liquid interface that is interacting with a Mach number 1.95 shock wave at x=3.025 initially in liquid. The initial conditions are: $\rho = 1, u = 0, v = 0, p = 1, \gamma = 1.4,$ for air, $\rho = 5, u = 0, v = 0, p = 1, \gamma = 4, B = 1,$ for pre-shocked liquid, $\rho = 7.093, u = -0.7288, v = 0, p = 10,$ $\gamma = 4, B = 1,$ for post-shocked liquid. The density field is shown in Fig. 11 where the complex wave structure is once again presented and is relatively well captured. To check the correctness of the results, in Fig. 12 we compare the distributions of density and pressure along y=0.5 at t=0.5 with the results ('$\circ$') in [7]. Good agreement of the solutions is clearly observed. Similar to the gas-gas interface, the relative mass error of the air medium is measured and shown in Fig. 13. The error by the WENO-FT method increases quickly after the shock wave transmits into the air medium and it shows that the RKDG-FT method has good behaviors for the mass conservation in this problem.

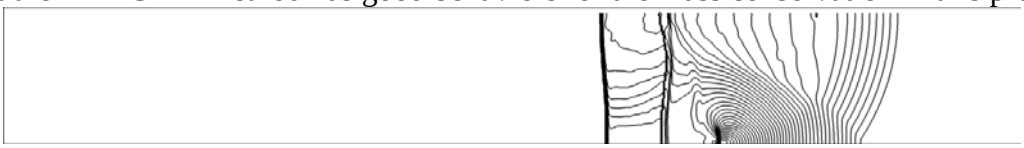

(a) t =0.3

(b) t =0.5

(c) t =1.0

Figure 11. Density field (100 equally spaced density contours from 0.5 to 7.5)

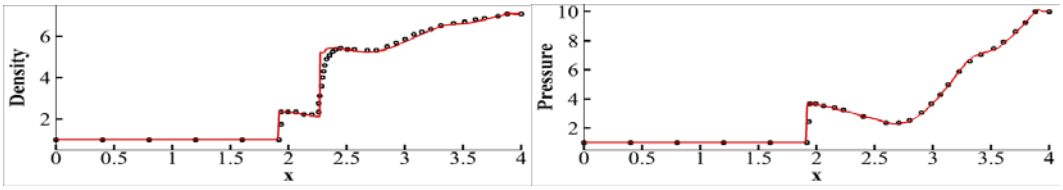

Figure 12. Comparison of density and pressure along y=0.5

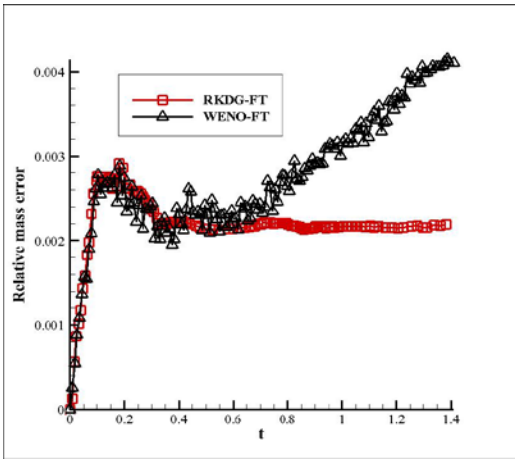

Figure 13. Comparison of relative mass error of air

Conclusions

In this paper, the RKDG method is applied to solve compressible two-medium flow. The interface is advanced by the front tracking method and the RGFM is used to define the interface boundary conditions. Due to the good compactness of the RKDG method, the ghost fluid states far from the interface which are less accuracy need not to be solved and used in the computation. Numerical results show that these procedures can work efficiently under different initial conditions. It also demonstrates that the RKDG-FT method has better mass conservation property compared to the WENO-FT method in general.

Acknowledgement

The research was supported by the National Basic Research Program of China ("973" Program) under grant No. 2014CB046200, NSFC grant 11432007.

References

[1] Cockburn, B. and Shu, C. -W. (1998) The Runge-Kutta discontinuous Galerkin method for conservation laws V: multidimensional systems, *Journal of Computational Physics* **141**, 199–224.

[2] Fedkiw, R. P., Aslam, T., Merriman, B., Osher, S. (1999) A non-oscillatory Eulerian approach to interfaces in multimaterial flows (the ghost fluid method), *Journal of Computational Physics* **152**, 457–492.

[3] Glimm, J., Grove, J. W., Zhang, Y. (2002) Interface tracking for axisymmetric flows, SIAM Journal on Scientific Computing **24**, 208-236.

[4] Lu, H. T., Zhao, N., Wang, D. H. (2016) A front tracking method for the simulation of compressible multimedium flows, Communications in Computational Physics **19**, 124-142.

[5] Lu, H. T., Zhu, J., Wang, D. H., Zhao, N. (2016) Runge-Kutta discontinuous Galerkin method with front tracking method for solving the compressible two-medium flow, Computers and Fluids **126**, 1-11.

[6] Lu, H. T., Zhu, J., Wang, C. W., Zhao, N. (2016) Runge-Kutta discontinuous Galerkin method with front tracking method for solving the compressible two-medium flow on unstructured meshes, Advances in Applied Mathematics and Mechanics (accepted).

[7] Shyue, K. -M. (1998) An efficient shock-capturing algorithm for compressible multicomponent problems, *Journal of Computational Physics* **142**, 208–242.

[8] Terashima, H., Tryggvason, G. (2009) A front tracking/ghost fluid method for fluid interfaces in compressible flows, *Journal of Computational Physics* **228**, 4012–4037.

[9] Wang, C. W., Liu, T. G., Khoo, B. C. (2006) A real ghost fluid method for the simulation of multimedium compressible flow, SIAM Journal on Scientific Computing **28**, 278–302.